A precise omegatron measurement of μ_p/μ_N

1974 J. Phys. A: Math. Nucl. Gen. 7 167

(http://iopscience.iop.org/0301-0015/7/2/002)

J. Phys. A: Math., Nucl. Gen., Vol. 7, No. 2, 1974. Printed in Great Britain.

A precise omegatron measurement of μ_p/μ_N

B W Petley and K Morris

Division of Quantum Metrology, National Physical Laboratory, Teddington TW11 0LW, UK

Received 20 August 1973

Abstract. The value obtained for the proton magnetic moment in nuclear magnetons was 2·792 774 8 ± 0·000 002 0 (0·72 ppm) without the diamagnetic shielding correction. Measurements were made with a quadrupole omegatron at flux densities of 0·47, 0·94 and 1·41 T. More than 400 sets of measurements were made using H_2^+, HD^+, D_2^+, $^4He^+$ ions and protons.

1. Introduction

The ratio of the magnetic moment of the proton μ_p to the nuclear magneton μ_N is measured experimentally by taking the ratio of the proton spin precession frequency f_s to its cyclotron frequency f_c in the same magnetic flux B (Alvarez and Bloch 1940), that is

$$f_s/f_c = \mu_p/\mu_N. \tag{1}$$

Determinations of μ_p/μ_N play an important part in the evaluation of the 'best values' of the fundamental constants of physics (Cohen and Dumond 1965, Taylor *et al* 1969). For many years the most precise determination was the omegatron measurement of Sommer *et al* (1951); but this value has recently been revised (Fystrom *et al* 1971). Other determinations were of broadly similar precision (Bloch and Jeffries 1950 (revised by Trigger 1956), Boyne and Franken 1961, Sanders and Turberfield 1963, Mamyrin and Frantsuzov 1965, 1968, Petley and Morris 1967, 1968, 1969). Since the 1969 review of the fundamental constants, several other values for μ_p/μ_N have been published (Fystrom 1970, 1971, Gubler *et al* 1971, Petley and Morris 1971, Luxon and Rich 1972, Mamyrin *et al* 1972a, b). These results were all higher than the value taken in the 1969 review but, with the exception of Mamyrin *et al*, the errors were all greater than 6 parts per million (ppm)†. The sub-ppm determination of Mamyrin *et al* (1972a, b) is 7 ppm lower than the result of Mamyrin and Frantsuzov (1965, 1968) which was largely neglected in the previous evaluations of the atomic constants, and is 23 ppm higher than the value recommended in the 1969 review. It was important therefore to obtain supporting evidence for the 1972 result by an independent method (Cohen and Taylor 1972).

We report here details of a new measurement of μ_p/μ_N which has an estimated precision of 0·72 ppm and supports Mamyrin's value. The determination was made with an improved version of our quadrupole omegatron (Petley and Morris 1965, 1967, 1968, 1969). The principal improvement is that the cyclotron resonances have been traversed by varying the applied radio frequency (Petley and Morris 1972a, b) and keeping the magnetic field constant rather than by scanning the magnetic field at constant

† Unless otherwise stated all errors quoted in this paper are estimated standard deviation uncertainties.

frequency. Measurements were made at flux densities of 0·47, 0·94 and 1·41 T. The new method has enabled the systematic errors to be investigated and eliminated with considerably greater precision than hitherto.

2. Theory of the quadrupole omegatron

The major difficulty with the omegatron method stems from the omegatron itself, since its electrodes must provide both a uniform radio frequency field and an electrostatic field which traps the ions in the magnetic field direction. Previous designs did not pay much attention to the trapping potential distribution. The form of this distribution is very important, for it determines the stability of the ion orbit and also causes shifts in the ion cyclotron frequency. Except in the simplest case, which our omegatron satisfies, the equations of motion of the ions can only be solved by approximate methods, and the use of such methods is not satisfactory in applications where the highest precision is required. Our design overcomes these difficulties and the theory of the operation of the quadrupole omegatron is given briefly below.

The ion trapping potential distribution satisfies the equation

$$\phi = V_T[k_0 - k_1(x^2 - z^2)] \tag{2}$$

where V_T is the applied ion trapping potential, k_0 and k_1 are geometric constants, the z axis is in the direction of the uniform magnetic flux B and the x axis is in the direction of the uniform radio frequency field $E_0 \sin(2\pi ft + \phi)$. The x, y, z origin is at the centre of the omegatron (see figure 2) and the axes form a right-handed set. The equations of motion of an ion of charge e and mass M are then:

$$M\ddot{x} = eE_0 \sin(2\pi ft + \phi) + eB\dot{y} + 2k_1 V_T ex \tag{3}$$

$$M\ddot{y} = -eB\dot{x} \tag{4}$$

$$M\ddot{z} = -2k_1 V_T ez. \tag{5}$$

The solutions to these equations are essentially the equiangular spirals that were obtained with the simple theories of the omegatron (Sommer 1950, Berry 1954, Brubaker and Perkins 1956), with the addition of a term $-(k_1 V_T e f_c / \bar{f}_c^2)(x_0 + V/2\pi f_c)t$ to the y solution, where at $t = 0$, we have $x = x_0$, and $\dot{y} = V$. This term represents drift of the orbit in the y direction with a uniform velocity. In addition the resonant frequency is shifted to $\bar{f}_c$ which is given exactly by

$$\bar{f}_c^2 = f_c^2 - \frac{k_1 V_T e}{2\pi^2 M}, \tag{6}$$

or

$$\bar{f}_c \simeq f_c - \frac{k_1 V_T}{2\pi B}. \tag{7}$$

The ions reach the collector when

$$\bar{f}_c - \tfrac{1}{2}\Delta f < f < \bar{f}_c + \tfrac{1}{2}\Delta f, \tag{8}$$

where the frequency width of the resonance is given by

$$\Delta f = \frac{E_0}{\pi B R_c}, \tag{9}$$

and R_c is the radius of curvature of the ion orbit at collection.

In principle the proton cyclotron frequency could be deduced by varying V_T and using equation (7), since the ratio of the ion mass to that of the proton is known with higher precision. Unfortunately any other radial electric fields in the omegatron, for example, space charge or contact potential variations, or effects from the electron acceleration and collection potentials etc, shift the frequency by a further amount which must be deduced experimentally, and equation (7) becomes

$$f_c = f_c - \delta f \tag{10}$$

where the shift δf must be determined experimentally. As with previous determinations, equations (1) and (10) lead to

$$(\mu_p/\mu_N)'' \simeq \mu_p'/\mu_N + \frac{\delta f}{f_s}(\mu_p'/\mu_N)^2 M/M_p \tag{11}$$

where

$$(\mu_p/\mu_N)'' = f_s/(f_c M/M_p) \tag{12}$$

and the spin precession frequency refers to protons in a spherically shaped water sample. Thus μ_p'/μ_N and δf_c may be obtained from the intercept and slope, respectively, of a least squares straight line fitted to the values of $(\mu_p/\mu_N)''$ as a function of M/M_p. The ion mass ratios are known with sufficient precision to be treated as auxiliary constants. It is a unique feature of our work that measurements of as many as five ion cyclotron frequencies, made in succession, were employed for fitting equation (11). The nuclidic mass values used were:

$$M(\mathrm{H}) = 1{\cdot}007\,825\,037\ \mathrm{u},$$

$$M(\mathrm{D}) = 2{\cdot}014\,101\,798\ \mathrm{u},$$

and

$$M(^4\mathrm{He}) = 4{\cdot}002\,603\,27\ \mathrm{u}.$$

(Wapstra *et al* 1972 private communication, 1974).

3. The apparatus

A block schematic diagram of the complete apparatus is given in figure 1.

3.1. The omegatron and vacuum system

The omegatron construction was similar to that used in our earlier determination, but with some important changes. The electrode and support wires were made from platinum–iridium (80/20) and the electrical connections were as indicated in figure 2. The values of k_0 and k_1 were again designed to be 0·5 and 0·5 cm^{-2} respectively and the plate separation was 2 cm. The length in the y direction was increased from 5 to 7·5 cm.

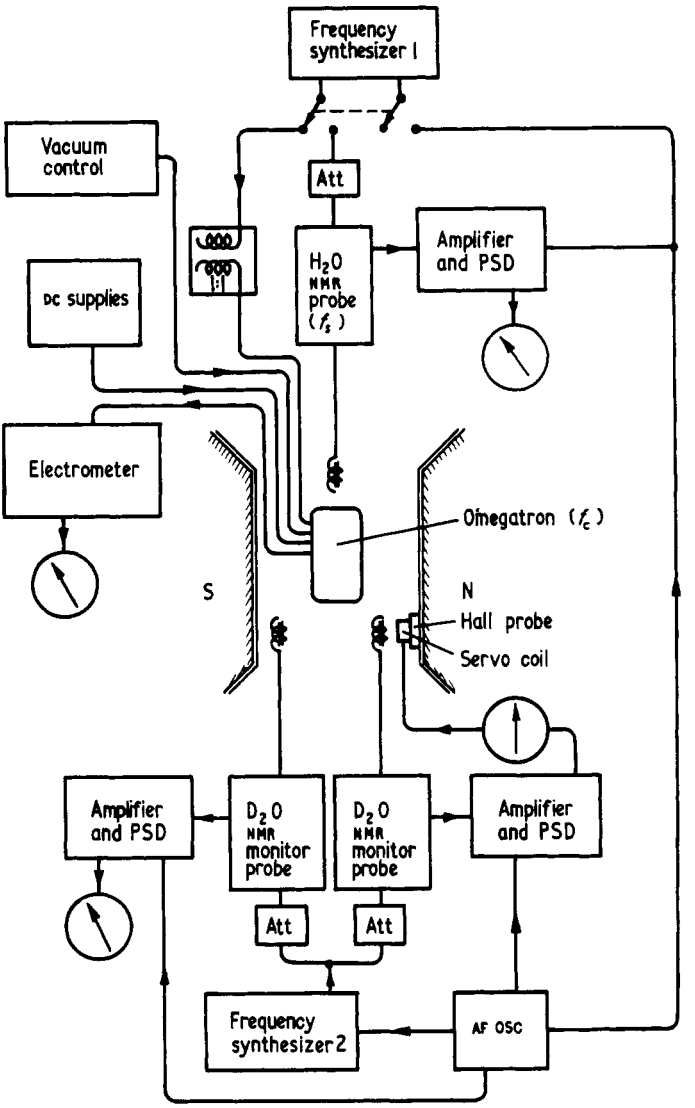

Figure 1. Block schematic diagram illustrating the overall arrangement of the equipment.

It was considered that there might be a contact potential difference between the conducting coating on the glass supporting end plates and the other electrodes, and so hyperbolic stars (shown by the dashed lines in figure 2 and clearly visible in the x ray photograph, figure 3) were placed over the end plates. A hole was made in one of them and covered with a cap, visible as an oval shape on the left hand side of the photograph, which could be pushed inwards for insertion of a small nuclear magnetic resonance probe on completion of the μ_p/μ_N measurements. The star shaped plates distorted the equipotentials by less than 10% and electrolytic tank studies showed that the effects were negligible a few millimetres from the end plates. Platinum was evaporated on to the inside surface of the containing glass cylinder and functioned as a further electrode. Ceramic rods were temporarily inserted during manufacture to ensure that the ion

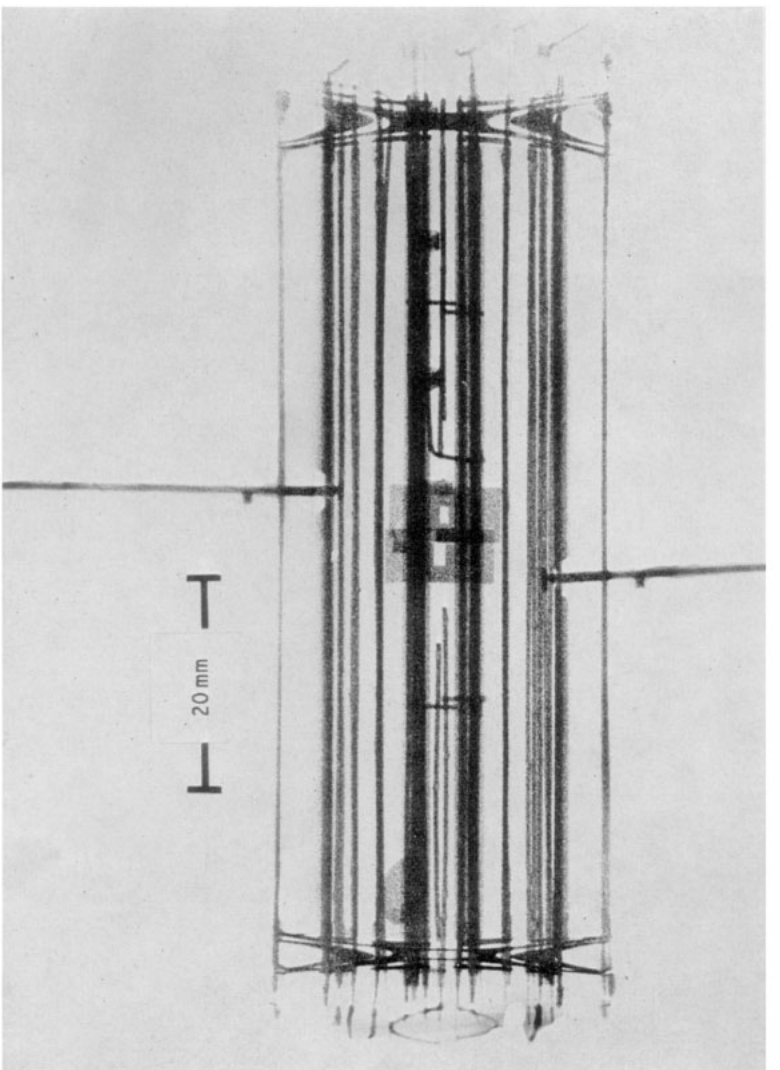

Figure 3. An x-ray photograph of the omegatron. The ion collector penetration was verified from this photograph. The hyperbolic stars used to cover the end plates and the hole for insertion of the NMR probe are also visible.

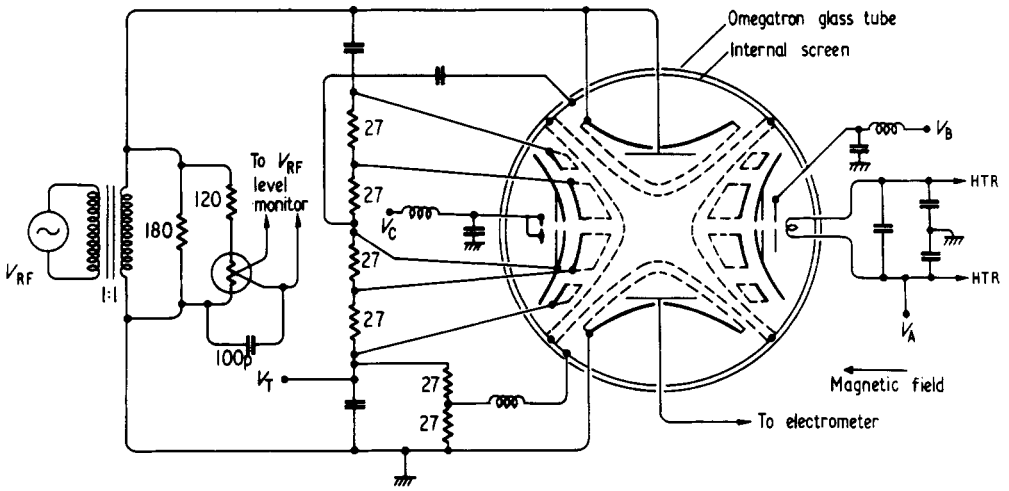

Figure 2. The electrode arrangement and method of making the connections to the quadrupole omegatron.

collector penetration was the design value of 1·5 mm and this penetration was checked at the completion of the measurements by using the x-ray photograph. The leads carrying the filament current were mounted close together to reduce the magnetic field effect.

After initial evacuation, the system was sealed off and a sputter ion pump used to obtain the lowest pressure and an evaporation ion pump used for the fine pressure control. Helium gas diffused through the glassware, while hydrogen and deuterium were produced by electrolysis and introduced through a heated silver–palladium leak.

3.2. The magnetic field

The magnetic field was produced by a commercial, 38 cm pole diameter, electromagnet with a Hall-probe stabilized power supply. The accessible air gap was 50 mm and the specified homogeneity was 1 ppm over a 2 cm cube at the design flux density of 1·4 T. The water cooling was controlled to 0·02°C and, after continuous running for about two days, the field was stable to better than 1 ppm over short periods. The field changes during a set of measurements of the ion cyclotron frequencies and spin precession frequencies are given in table 1. Each set took about 12 minutes to obtain. The spin precession frequencies were measured by a substitution interchange at the beginning and end of each set and the four or five ion cyclotron frequencies were measured in the intervening 8 minutes.

For the sets in groups 2 and 3 in table 2, the field was stabilized by a deuterium NMR probe (figure 1), the output from the phase sensitive detector being passed through a small coil placed over the Hall-effect probe, giving a stability factor of about six. A second deuterium NMR probe served to check that the field remained locked to the NMR signal.

A point by point calibration plot of the magnetic field was made daily for the results in groups 3, 4 and 5, and less frequently for the earlier groups; it was found that the variations from one plot to another were small. A contour fitting program was used to interpolate the measured points and the number of measurements required for an

Table 1. Table of the measured and estimated magnetic field dependent parameters, figures in parenthesis represent the standard deviation uncertainties in the last two digits quoted

Parameter	Unit	Proton spin precession frequency		
		20 MHz (0·47 T)	40 MHz (0·94 T)	60 MHz (1·41 T)
Partial pressure frequency shift	10^{14}Hz A^{-1}	0·0302(91)	0·0516(93)	0·0799(113)
Half-height resonance width				
Experimental values	kHz V_{RMS}^{-1}	6·24(9)	3·14(2)	2·08(2)
Experiment/theory	—	1·171(17)	1·180(7)	1·171(11)
Frequency shift with trapping voltage				
Experimental values	kHz V^{-1}	1·553(226)	0·944(37)	0·589(3)
Experiment/theory	—	0·917(133)	1·114(43)	1·054(4)
'Shielding' effect				
(i) Omegatron	ppm	1·85(10)	2·10(4)	1·68(3)
(ii) Single perspex sheet	ppm	−0·81(6)	−1·07(18)	−0·85(5)
(iii) Double perspex sheet	ppm	−1·85(11)	−2·35(10)	−1·63(8)
Filament current effect: (+)-(−)	ppm	9·14(188)	3·83(29)	2·25(15)
Field inhomogeneity (σ)	ppm	0·9	0·8	0·15
Relativistic shift in proton cyclotron frequency	Hz	3·27	26·13	88·18
Relativity error	ppm	0·01	0·04	0·1
Magnetic field change while runs were being obtained				
Mean	ppm	0·08	0·16	0·01
σ_{single}	ppm	0·30	0·51	0·12

interpolation precision of better than 0·1 ppm was established experimentally. In fact, the values measured at the beginning and end of each set of measurements of f_c were within 0·2 ppm of the average obtained from the field plot.

4. Measurement of the ion cyclotron frequencies

Although a rectangular shaped resonance curve might be expected from the simple theory, in practice a trapezoidal shaped resonance was observed. This was simply a consequence of the finite size of the electron beam producing the ions. Thus the radius of curvature R_c of the ion orbit varied by 0·5 mm (in 9 mm) in going from the base to the top of the resonance and consequently so did the frequency width as shown in equation (9). The use of trapezoidal resonances allows ion masses to be distinguished well within the limits set by the usual definitions of resolving power. This is demonstrated in figure 4 where the ions CH_3^+ and CHD^+ are clearly distinguishable.

The use of trapezoidal resonances meant that some restrictions were placed on the operating conditions, essentially allowing only a limited amount of orbit drift. These were (i) a lower limit to the RF level which varied linearly with the ion trapping voltage,

Table 2. Table summarizing the values obtained for μ_p'/μ_N. The values in parenthesis are the standard deviation uncertainties in the last two digits quoted. The criterion for a 'poor' run was a large scatter of the points about the fitted straight line, as indicated by the standard deviation of the intercept. σ_B is a measure of the precision with which f_s/f_c was estimated for one group relative to another and was included as an error in obtaining the 'weighted mean'

f_s	Group	Number of runs	Number of 'poor' runs	Ions used for fitting lines	σ_B(ppm)	Value of μ_p'/μ_N	
						All runs	Without 'poor' runs
60 MHz	1	89	6	H_2^+, HD^+, D_2^+, $^4He^+$	0·5	2·792 775 74(42)	2·792 775 27(40)
	2	145	7	H_2^+, HD^+, D_2^+, $^4He^+$	0·3	774 30(30)	774 54(24)
	3	71	4	H^+, H_2^+, HD^+, D_2^+, $^4He^+$	0·15	774 74(72)	773 44(35)
	3	82	5	H_2^+, HD^+, D_2^+, $^4He^+$	0·15	775 21(28)	774 98(21)
40 MHz	4	38	2	H^+, H_2^+, HD^+, D_2^+, $^4He^+$	0·8	774 74(72)	773 10(27)
	4	40	2	H_2^+, HD^+, D_2^+, $^4He^+$	0·8	772 90(44)	773 24(34)
20 MHz	5	33	2	H^+, H_2^+, HD^+, D_2^+, $^4He^+$	0·9	776 00(267)	776 49(192)
	5	40	2	H_2^+, HD^+, D_2^+, $^4He^+$	0·9	774 92(372)	776 75(265)
		Weighted mean				774 97(40)	774 65(38)

(ii) a lower limit to the trapping voltage which was set purely by the thermal energy of the ions which would otherwise allow them to escape in the magnetic field direction. There was also an upper limit to the RF amplitude of 1 V (RMS) which was determined in part by the RF source and also by the decreasing precision with which the centre of the resonance could be estimated as the RF level, and hence frequency width, increased. Within these operating restrictions the scale, but not the shape of the resonances, changed with the amplitude of the RF field and the shapes were independent of ion mass as expected from equation (9). Measurements were usually made at the resonance half-height points. Changes in the applied radio frequency of one hertz caused perceptible level changes at the half-height point, where the slope was steepest. Further measurements were also made near the base and top of the resonances to investigate any mass dependent changes of the cyclotron frequency with height, which could cause μ_p/μ_N to vary similarly. In contrast with our earlier determination there was only a small variation of less than or equal to 5 Hz from base to top, which is accounted for by small non-uniformities in the magnetic and electrostatic fields and changes in the relativistic effects.

The frequency scanning method had a considerably greater precision than magnetic scanning of the resonance and so a number of performance checks were required which are described in the following sections.

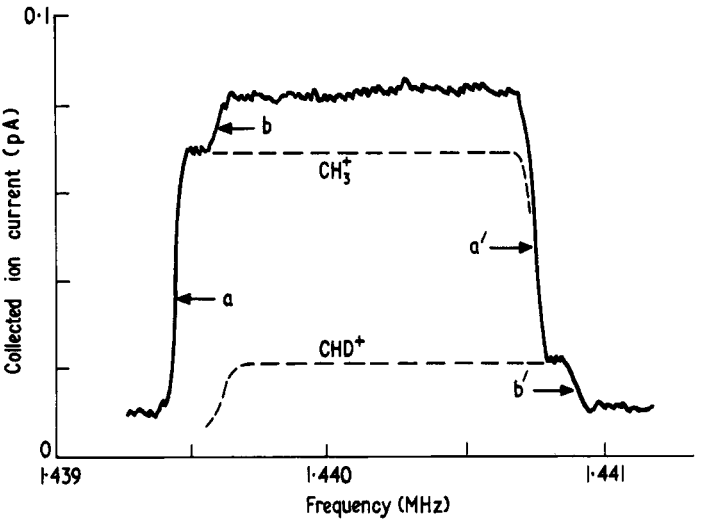

Figure 4. Example of unresolved but distinguishable trapezoidal shaped resonances at mass 15 (taken at 1·41 T, 19μN m^{-2}, V_{RF} = 0·6 V, V_T = 0·6 V and 1μA electron current). The mass difference $\delta M_u/M_u$ is 1 in 10^4 and the resolving power $\Delta f_c/f_c$ is 1 in $1{\cdot}2 \times 10^3$. Measurements at the half-height points a–a', b–b' were consistent with those made of the lighter mass ions.

4.1. Constancy of the radio frequency amplitude

The RF source was a mains stabilized, 10 kHz to 100 MHz frequency synthesizer and power amplifier. The RF levels were set to 0·1 dB using a switched attenuator. Careful attention was paid to impedance matching, particularly at the omegatron. A DC-calibrated UHF vacuum thermo-junction was connected to the base of the omegatron and used to monitor the RF level. As is evident from equations (8) and (9), any change in the RF level could cause a distortion of the centre frequency, but a linear variation would simply lead to a mass independent frequency shift, adding to δf in equation (10) and hence would not affect the value of μ_p/μ_N. It was established that the amplitude changes were less than 0·1 % per 10 kHz change, which would affect the values at 1·41 T by less than 0·1 ppm. As a check the cyclotron frequencies of H_2^+ and $^4He^+$ ions were compared when the RF level was changed from 0·5 to 1·0 V (RMS) and they each changed by about 2 Hz. Such a change would not affect the value of μ_p/μ_N and, although it might be an effect of the RF field (arising, for example, from the effects of any non-uniformities in the RF field), it was probably a result of the ions averaging the residual electrostatic fields differently as the RF level was changed.

As expected, the standard deviation of the measured frequencies about the fitted lines to equation (11) increased with the RF level. Consequently it was difficult to establish that the value of μ_p/μ_N did not depend on the RF level. In addition there were possible effects due to non-uniformities in the RF field. An approximate analysis indicated that in the first order the effect would be mass independent and so would not affect the value obtained for μ_p/μ_N. The error assigned for the possible effect of the RF level (table 4) was 0·3 ppm.

4.2. Resonance width

The variation of the resonance width with RF level and magnetic field was investigated

and was found to be independent of the mass of the ion studied, as expected from equation (9). The results are summarized in table 1. To obtain the theoretical estimate, E_0 was assumed to be equal to the RF amplitude divided by the distance between the plates. However, the perturbing effect of the ion collector and the method of generating the RF field probably accounted for the slightly broader resonances that were observed experimentally. The resonance widths depended slightly on the trapping voltage, through orbit drift which affected the value of R_c, and also on the filament current direction. The latter was a small mass dependent effect of about 5 Hz which averaged to zero when the filament current direction was reversed.

4.3. Effect of the ion trapping voltage

The frequency changes with the ion trapping voltage were found to be mass independent and in good agreement with the linear relationship expected from equation (7). The results are summarized in table 1. The weighted mean ratio of the experimental to theoretical frequency shift was $1{\cdot}043 \pm 0{\cdot}004$. The small difference from unity is interpreted to be a consequence of the truncation of the hyperbolic surfaces, which led to a slight increase in the value of k_1 in equation (2).

4.4. Effect of the space charge and inequalities in the ion currents

Measurements of the frequency shifts were made for system pressures between 3·5 and 107 $\mu N\,m^{-2}$ and the results were compatible with $0{\cdot}712 \pm 0{\cdot}06$ Hz per $\mu N\,m^{-2}$. The average operating pressure for the μ_p'/μ_N results was $13{\cdot}3\,\mu N\,m^{-2}$ so that the total frequency shifts due to ion space charge amounted to only 9·5 Hz at 1·41 T (see discussion in § 6).

The collected ion current varied according to the mass of the resonant ion since it was not possible to make the partial pressures exactly the same. There was consequently the possibility that the frequency shift resulting from the ion space charge would vary when different ions were at resonance. This effect was investigated by measuring the difference between the ^4He and D_2 cyclotron frequencies as a function of the difference between the collected ion currents. A small effect was found which was compatible with a linear relationship between the cyclotron frequency and ion current. The slopes of the fitted least squares straight lines are given in table 1 and were used to correct the measured ion cyclotron frequencies. The corrections were in practice quite small, for example at 1·41 T they averaged only $0{\cdot}96 \pm 0{\cdot}69$ Hz, but their effect has been included in the error assignment.

The intercepts corresponding to equal collected ion currents were used to obtain a value for the $D_2 - {}^4He$ mass difference. The value obtained was $25\,600{\cdot}3 \pm 0{\cdot}3$ μu, which may be compared with the latest nuclidic mass table value of $25\,600{\cdot}323 \pm 0{\cdot}063$ μu. The values are in excellent agreement and provide a further check of the precision of the omegatron.

4.5. Dimensionless parameters

In addition to the $D_2 - {}^4He$ mass difference mentioned in the previous section, two dimensionless parameters were calculated from the experimental results as shown in table 3. These parameters involve the ratio of differences between ion cyclotron frequencies and so may be compared with the values derived from nuclidic mass tables.

Table 3. Comparison between the experimental and theoretical values of the two dimensionless parameters. Numbers in parenthesis are standard deviation errors in the last digits quoted. The nuclidic mass values are believed to be accurate to rather better than the last digit quoted

Magnetic field in terms of f_s(MHz)	Dimensionless parameters	
	$\frac{3(f_c(H^+)-f_c(HD^+))}{8(f_c(H_2^+)-f_c(^4He^+))}$	$\frac{3(f_c(H^+)-f_c(HD^+))}{8(f_c(H_2^+)-f_c(D_2^+))}$
20	1·007 282 2 (24)	1·000 829 4 (20)
40	1·007 282 4 (1)	1·000 830 8 (1)
60	1·007 282 5 (4)	1·000 831 0 (4)
Value from nuclidic mass tables	1·007 282 3	1·000 830 8

It can be seen that the agreement is excellent. These parameters are a particularly sensitive test of the relativistic correction.

4.6. Relativistic correction

The ions gain sufficient energy from the RF field for their mass to be increased slightly by relativistic effects. Consequently a slightly lower radio frequency is required to accelerate the ions. Thus the instantaneous cyclotron frequency becomes

$$\bar{f}_c' = \bar{f}_c[1-(2\pi r\bar{f}_c/c)^2]^{1/2} \tag{13}$$

where c is the speed of light and r is the radius of curvature of the ion orbit. Equation (13) approximates to

$$\bar{f}_c' = \bar{f}_c - 2\pi^2\bar{f}_c^3 r^2/c^2 \tag{14}$$

which suggested that the overall shift in the cyclotron frequency would depend on the mean square radius of curvature of the ions. A more rigid analysis, involving the approximate solution of the relativistic differential equation:

$$\frac{d}{dt}(k^{-1/2}\dot{r}) = \frac{eE_0}{M}\sin(2\pi ft+\phi) - i2\pi f_c\dot{r} \tag{15}$$

(where $r = x+iy$ and $k^{1/2} = \bar{f}_c'/\bar{f}_c$) confirmed this conclusion. The mean square radius of curvature of the ions varied from $\frac{1}{3}R_c^2$ at the centre to $\frac{1}{2}R_c^2$ at the edge of the resonance.

The value of this correction was checked by omitting the correction and fitting an appropriate curve through the measured cyclotron frequencies instead of equation (11). This enabled the value of R_c to be deduced via the relativistic effects. The values obtained were $9{\cdot}2\pm0{\cdot}2$ and $8{\cdot}8\pm0{\cdot}3$ mm at 1·41 and 0·94 T respectively. The design value was $9\pm0{\cdot}5$ mm and hence the assigned relativistic correction is believed to be close to the true one. The assigned error in table 1 corresponds to the change in the value of μ_p'/μ_N if R_c is changed by 0·5 mm.

4.7. The filament current effect

The direct current of about 1·5 A used to heat the tungsten filament shifted the cyclotron frequency and a number of measurements were made to confirm that the shift was

consistent with the heater current producing a small perturbing magnetic field. The effect in the present omegatron was half that in the previous version and effectively changed the spin precession frequency inside the omegatron by $72{\cdot}0 \pm 3{\cdot}8$ Hz. This value was inferred from the mass-dependent changes in the ion cyclotron frequencies when the heater current was reversed at 0·47, 0·94 and 1·41 T. Confirmatory evidence was obtained by using small NMR probes located outside the omegatron during the experiment and another probe which was mounted inside it at the completion of the μ_p'/μ_N measurements. These probes showed that the field reversed, to within 1 Hz in 60 MHz, when the current direction was reversed and that the effect varied linearly with the heater current. Thus any movement of the filament under the force from the interaction of the magnetic field with the heater current produced a negligible effect. When the current was increased until the electron beam current was five times the usual value, some hysteresis was found, which at that current would have caused a 0·1 ppm error in the value of μ_p'/μ_N.

The upper limit to the space charge change on reversal was investigated by measureing the change in the ion cyclotron frequency and corresponded to about 5 Hz at 1·41 T. This limit was difficult to establish because reversing the heater current meant switching it off, with a consequential change in the system pressure, and also because the heater current was always brought slowly to the working value to avoid temperature overshoot. It was concluded that at the present precision the filament current effect was compatible with a purely magnetic effect which reversed with the heater current direction.

5. Measurement of the spin precession frequency

The proton spin precession frequency was measured with an unshielded NMR probe using the amplitude bridge method (Thomas and Huntoon 1949). The same frequency synthesizer was used to measure both the ion cyclotron and proton spin precession frequency. The frequency was modulated at 20 Hz to a depth of a few hertz and checks were made with another probe using magnetic field modulation to verify that there was no distortion of the resonance—the two methods agreed to 2 Hz in 60 MHz. The effects of changing the RF level or detuning the probe by as much as 50% were also found to be negligible under the experimental conditions that were finally adopted, namely the low RF and modulation levels and small sized samples.

Measurements with probes of different size suggested that the probe diameter should be as small as possible. Several probes were used but they were all finally referred to a 1·65 mm diameter probe which contained pure water. The probe length was 75 mm and the wall thickness was 0·08 mm. Measurements with different probes by the substitution method suggested a precision of 0·1 ppm.

5.1. Substitution correction

The proton spin precession frequency was measured during the experiment by means of a small NMR probe which was attached to the omegatron. The omegatron was moved before and after each set of f_c measurements so that the NMR probe occupied the same position in the pole gap as the centre of the omegatron. At the conclusion of the μ_p'/μ_N measurements the NMR probe, mentioned above, was inserted into the omegatron and the difference between the fields experienced by the two probes was measured. It was found that the field was slightly greater inside the omegatron than outside, the amounts

changing with field as given in table 1. The change was quite repeatable and did not vary with the speed of movement of the omegatron over a range five times slower to five times faster than the usual speed. The value was the same in different parts of the magnet gap and repeated after the magnet had been switched off and on.

Measurements were also made with other materials which suggested that the main cause of the change was due to the material of the omegatron affecting the value of the field locally. A diamagnetic material decreased the field and a paramagnetic material increased the field. Theoretical consideration suggested that a material of thickness t, susceptibility χ, placed in the air gap d, changed the field by a fraction $\chi t/d$. The field changes caused by the insertion of two pieces of perspex sheet into the pole gap ($114 \times 45 \times 6{\cdot}3$ mm^3, susceptibilities $-0{\cdot}65$ and $-0{\cdot}69 \times 10^{-8}$ kg^{-1} at 20 °C respectively) were measured. The results, given in table 1, are in good agreement with the theoretical values of $-0{\cdot}87$ and $-1{\cdot}79$ ppm respectively. The values also changed with magnetic field in a similar way to that found with the omegatron. It is considered therefore that the substitution and shielding correction is reasonably well understood at the present precision. The assigned error of 0·25 ppm takes into account the fact that the correction was assumed to apply throughout the measurements. These findings have implications for other experiments which involve substitution measurements of magnetic fields in electromagnets or permanent magnets which have a comparatively small air gap.

6. Results

The major advantage of the omegatron method is that it is possible to investigate the effect of varying the operating conditions. Aside from the pressure variations mentioned earlier, the trapping voltage was varied between 0·2 and 3 V, the RF voltage from 0·5 to 1 V (RMS), the electron current from 0·5 to 2 μA while the electron acceleration and collection potentials were also changed.

The results of the measurements with frequency scanning are given in table 2 and were taken over a period of about a year. The results are divided into groups appropriate to the precision at the time that they were measured. To arrive at a weighted mean from these it is necessary to allow for the poorer magnetic field uniformity at the lower fields. We have taken the values given in table 1 which are equal to $\frac{1}{6}$ the RMS deviation of the magnetic field values at the edge of the ion orbit from that at the centre.

The results have been evaluated with and without the runs which we have termed 'poor' runs. These runs were characterized by the scatter of the measured cyclotron frequencies about the fitted lines, equation (11), as measured by the standard deviation of the intercept which was computed for each fitted line. The distribution of these standard deviations for each group are shown in figure 5 and are of the form expected for one degree of freedom; the improvement from one group to another is apparent. In group 1, one run in three had a σ_I greater than 1·8 ppm whereas in group 3 this was reduced to one in sixteen runs. The distribution of the μ'_p/μ_N values for these runs are shown in figure 6 and those having $\sigma_I > 10^{-5}$ (3·6 ppm) are shown as the shaded values. It is evident that the latter tended to lead to values of μ'_p/μ_N which were some way from the mean. It was decided therefore to use the value of σ_I as an indication of the quality of a run, for groups 1, 2, 4 and 5 the criterion was $\sigma_I > 2 \times 10^{-5}$ (7·2 ppm) and for group 3 $\sigma_I > 10^{-5}$. The difference between the results with and without these runs is only 0·11 ppm and is mainly important for deciding the last digit of the final value. The value that we have given is midway between the two values.

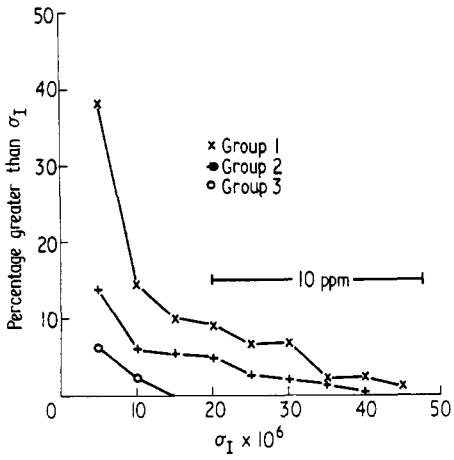

Figure 5. Showing the quality of the measurements improving with time. The 'quality' being defined by the standard deviation of the intercept calculated for each least squares fitted straight line.

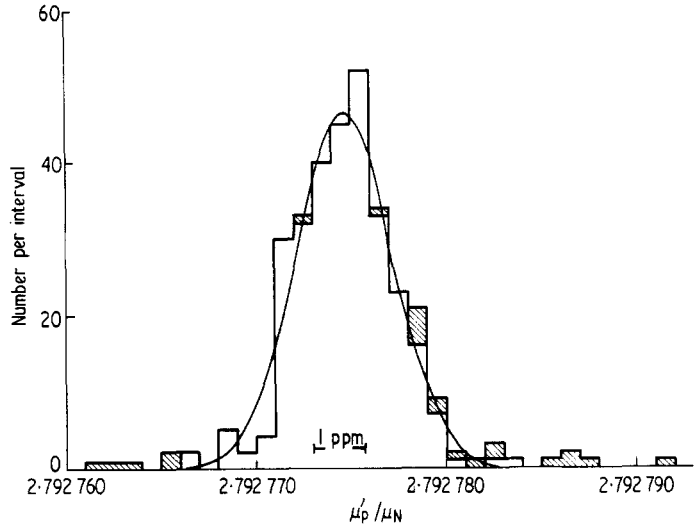

Figure 6. The overall distribution of the μ_p'/μ_N results obtained at 1·41 T (f_s = 60 MHz) H_2^+, HD^+, D_2^+ and $^4He^+$ ions. The shaded areas represent the runs having $\sigma_I > 10^{-5}$ (see figure 5). The distribution without the shaded runs is quite well represented by the fitted normal distribution (mean 2·792 774 7, standard deviation $2{\cdot}496 \times 10^{-6}$, χ^2 = 8·72 for 7 degrees of freedom).

It is concluded that there is no evidence of a significant variation of the value of μ_p'/μ_N with magnetic field. In arriving at this conclusion we have taken into account indirect evidence such as the dimensionless parameters and the values given in table 1. A further consideration is that in evaluating the magnetic field correction it was assumed that the ions were on the average collected after a drift of about 2 mm. If they are assumed to have been collected from a point opposite the ion collector the 60 MHz value would

be increased by 0·08 ppm and the 20 and 40 MHz value by 0·5 ppm. Orbit drift was of course greater at the lower magnetic fields.

The most important parameter was found to be the operating pressure. Results became unreliable above 40 $\mu N\,m^{-2}$ and it was necessary to wait for an hour or two for the pressure conditions to stabilize—indeed this was the probable cause of the 'poor' runs. It was concluded that there was some gas absorption on the electrode surfaces which took some time to stabilize. Occasionally the resonances were found to be two-valued in their width. The most likely explanation for this effect, which was not repeatable, appeared to be contact potential variations over the electrode surfaces, for the effect disappeared following a system bake-out. These effects were usually most serious when the operating conditions were close to those at which the resonances began to lose their trapezoidal shape; that is, where the orbit drift was greatest.

6.1. Magnetic field scanning

As a check 60 sets of resonances were obtained at 1·41 T, with magnetic field scanning, using H_2^+, HD^+, D_2^+ and $^4He^+$ ions, and the resulting value for μ'_p/μ_N was

$$2{\cdot}792\,776\,1 \pm 0{\cdot}000\,014\,(5\text{ ppm}).$$

Our preliminary value (Petley and Morris 1971) should be revised upwards by 3·53 ppm. This change results from using the latest nuclidic mass value for ^4He, the true omegatron 'shielding' correction (which was not known at the time) and the discovery of an error in the assigned magnetic field correction. The revised value is

$$2{\cdot}792\,764\,1 \pm 0{\cdot}000\,023\,(8{\cdot}2\text{ ppm}).$$

7. Discussion

The overall assessment of the systematic errors is summarized in table 4 and these have already been discussed in the relevant sections of this paper. They are estimated to be

Table 4. Table of the errors assessed as standard deviations. These are all systematic errors with the exception of the statistical error, which is that appropriate to the weighted mean

Source of error	ppm	$(ppm)^2$
Independence of trapping voltage	0·20	0·040
Independence of system pressure	0·30	0·090
Independence of ion partial pressure	0·10	0·010
Dependence on height up the resonance	0·20	0·040
Independence of RF amplitude	0·30	0·090
Elimination of filament current effect	0·15	0·023
Relativistic correction	0·25	0·063
Independence of magnetic field	0·20	0·040
Substitution and shielding error	0·25	0·063
Overall measurement of f_s	0·20	0·040
Nuclidic mass error	0·03	0·009
Frequency measurement	0·05	0·003
Statistical error	0·14	0·020
Root sum squares	0·72	0·520

standard deviation uncertainties and are, with one exception, systematic errors. The overall error is not much smaller than the standard deviation of a single set of measurements despite the fact that more than 400 sets of measurements were made. This reflects the difficulty of eliminating conclusively possible systematic effects. On the basis of these measurements we conclude that our best value for μ'_p/μ_N is

$$2{\cdot}792\,774\,8 \pm 0{\cdot}000\,002\,0\ (0{\cdot}72\ \text{ppm}),$$

without the diamagnetic shielding correction for a spherically shaped pure water sample at 25 °C. (A change of 5 °C in the laboratory temperature would only change the result by one digit in the last decimal place.)

Our result is less than 0·5 ppm higher than the only other measurement having an estimated standard deviation of less than a part in a million (Mamyrin *et al* 1972a, b) and the good agreement with other recent measurements which have a precision of around 6 ppm is evident in figure 7. The results are some 23 ppm higher than those of the 1969 evaluation and consequently there will be considerable changes in the values of many atomic constants in the next review (Cohen and Taylor 1973).

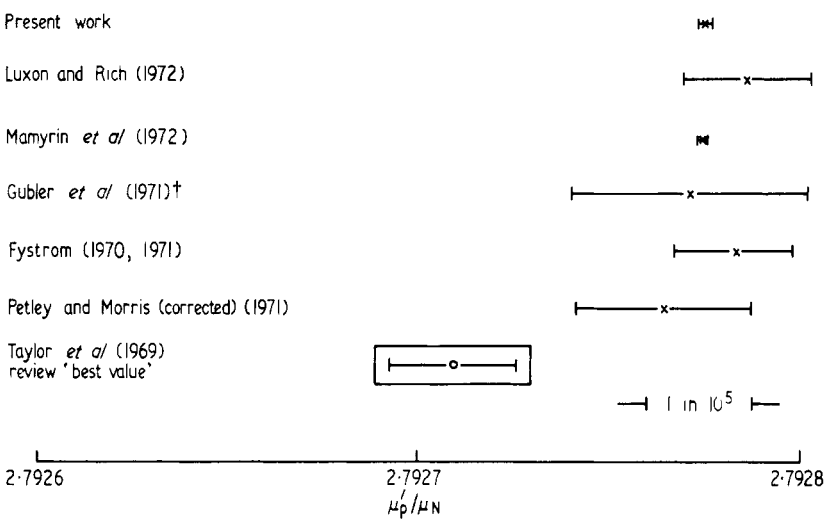

Figure 7. Measurements of μ_p/μ_N since the 1969 review.

Note added in proof. Gubler, Münch and Staub (to be published) have given a final value of 2·792 777 ($\pm$7 ppm) which is 2 ppm higher than the value plotted in figure 7.

References

Alvarez L W and Bloch F 1940 *Phys. Rev.* **57** 111–22
Berry C E 1954 *J. appl. Phys.* **25** 28–31
Bloch F and Jeffries C D 1950 *Phys. Rev.* **80** 305–6
Boyne H S and Franken P A 1961 *Phys. Rev.* **123** 242–54
Brubaker W M and Perkins G D 1956 *Rev. sci. Instrum.* **27** 720–5
Cohen E R and Dumond J W M 1965 *Rev. mod. Phys.* **37** 537–94

† See note added in proof.

Cohen E R and Taylor B N 1972 *Atomic Masses and Fundamental Constants 4* ed J H Sanders and A H Wapstra (London: Plenum) pp 543–63
—— 1973 *J. Phys. Chem. Ref. Data* **2** to be published
Fystrom D O 1970 *Phys. Rev. Lett.* **25** 1469–72
—— 1971 *Precision Measurements and Fundamental Constants* (NBS Special Publication 343) ed D N Langenberg and B N Taylor (Washington: USGPO) pp 169–72
Fystrom D O, Petley B W and Taylor B N 1971 *Precision Measurements and Fundamental Constants* (NBS Special Publication 343) ed D N Langenberg and B N Taylor (Washington: USGPO) pp 187–91
Gubler H, Reichart W, Roush M, Staub H and Zamboni F 1971 *Precision Measurements and Fundamental Constants* (NBS Special Publication 343) ed D N Langenberg and B N Taylor (Washington: USGPO) pp 177–85
Luxon J L and Rich A 1972 *Phys. Rev. Lett.* **29** 665–8
Mamyrin B A, Aruyev N N and Alekseenko S A 1972a *Zh. eksp. teor. Fiz.* **63** 3 (1973 *Sov. Phys.–JETP* **63** 1–9)
—— 1972b *Atomic Masses and Fundamental Constants 4* ed J H Sanders and A H Wapstra (London: Plenum) pp 451–6
Mamyrin B A and Frantsuzov A A 1965 *Zh. eksp. teor. Fiz.* **48** 416–28 (1965 *Sov. Phys.–JETP* **21** 274–82)
—— 1968 *Proc. 3rd Int. Conf. on Atomic Masses* ed R C Barber (Winnipeg: University of Manitoba Press) pp 427–36
Petley B W and Morris K 1965 *J. sci. Instrum.* **42** 492–4
—— 1967 *Nature, Lond.* **213** 586
—— 1968 *Proc. 3rd Int. Conf. on Atomic Masses* ed R C Barber (Winnipeg: University of Manitoba Press) pp 461–75
—— 1969 *National Physical Laboratory Report* QU7
—— 1971 *Precision Measurements and Fundamental Constants* (NBS Special Publication 343) ed D N Langenberg and B N Taylor (Washington: USGPO) pp 173–5
—— 1972a *Atomic Masses and Fundamental Constants 4* ed J H Sanders and A H Wapstra (London: Plenum) pp 445–50
—— 1972b *Nat. Phys. Sci.* **240** 83–4
Sanders J H and Turberfield K C 1963 *Proc. R. Soc.* A **272** 79–101
Sommer H 1950 *PhD Thesis* Agricultural and Mechanical College of Texas
Sommer H, Thomas H A and Hipple J A 1951 *Phys. Rev.* **82** 697–702
Taylor B N, Parker W H and Langenberg D N 1969 *Rev. mod. Phys.* **41** 375–496
Thomas H A and Huntoon R D 1949 *Rev. sci. Instrum.* **20** 516–20
Trigger K R 1956 *Bull. Am. Phys. Soc.* II **1** 220
Wapstra A H, Gove N B and Bos K 1974 to be published